Optics Letters

Demonstration of a 10 Mbit/s quantum communication link by encoding data on two Laguerre–Gaussian modes with different radial indices

Kai Pang,[1,*] Cong Liu,[1] Guodong Xie,[1] Yongxiong Ren,[1] Zhe Zhao,[1] Runzhou Zhang,[1] Yinwen Cao,[1] Jiapeng Zhao,[2] Haoqian Song,[1] Hao Song,[1] Long Li,[1] Ari N. Willner,[1] Moshe Tur,[3] Robert W. Boyd,[2] and Alan E. Willner[1]

[1]Department of Electrical Engineering, University of Southern California, Los Angeles, California 90089, USA
[2]Department of Physics and Astronomy, The Institute of Optics, University of Rochester, Rochester, New York 14627, USA
[3]School of Electrical Engineering, Tel Aviv University, Ramat Aviv 6997801, Israel
*Corresponding author: kaipang@usc.edu

Received 6 August 2018; revised 14 October 2018; accepted 18 October 2018; posted 26 October 2018 (Doc. ID 341638); published 14 November 2018

We experimentally demonstrate a 10 Mbit/s free-space quantum communication link using data encoding on orthogonal Laguerre–Gaussian (LG) modes with the same azimuthal index but different radial indices. Data encoding on two $LG_{\ell p}$ modes (i.e., for $\ell = 0$, we encode ["0", "1"] as [$p = 0$, $p = 1$], and for $\ell = 1$, we encode ["0", "1"] as [$p = 0$, $p = 1$]) is demonstrated by employing directly modulated laser diodes and helical phase holograms. The quantum symbol error rate (QSER) of <5% is achieved at an encoding rate of 10 Mbit/s. Moreover, the influence of the circle radius (R) of the receiver phase pattern on registered photon rates and QSERs is investigated. Our results show that a receiver phase pattern whose R does not match the beam size of the LG modes would induce higher cross talk between the two encoded quantum branches.

https://doi.org/10.1364/OL.43.005639

Quantum optical communication links have the potential for enhanced system security [1–5]. Typically, a quantum communication link employs two orthogonal states, such as the polarization of a photon for data encoding. In such a quantum qubit system, only one bit of information is encoded on each photon. An increase in the number of orthogonal states in a quantum communication link could potentially improve both its security and photon efficiency (e.g., bits/photon) [6–9].

One potential technique to achieve a larger alphabet is to employ a set of multiple orthogonal spatial modes from a modal basis set for quantum data encoding. The orthogonality would enable the selection of the desired mode at the receiver with little inherent cross talk to other quantum states [10,11]. In this case, each photon occupies only one of the d orthogonal spatial modes at a given time slot, where d is the number of possible states that are used for encoding. Compared with a conventional qubit system where only two orthogonal states are available, this higher dimensional qubit system might potentially provide a photon efficiency of up to $\log_2(d)$ bits per photon [10–14].

One example of a possible spatial basis set is Laguerre–Gaussian (LG) modes, which can be characterized by two indices: the azimuthal index ℓ and the radial index p [15,16]. LG modes with different ℓ values or p values are orthogonal with each other. In the classical domain, mode multiplexing (i.e., each mode carries an independent data stream) and data encoding (i.e., each pulse occupies a given LG mode state) using different ℓ or p values have been demonstrated [17–22].

In the quantum domain, a single photon can occupy a given quantum state; for an LG basis set, a given ℓ and p value would represent the state [23–25]. Previously, there have been several demonstrations of data encoding on the same p and different ℓ values [13,14,24,26]. To the best of our knowledge, there have been few reports of quantum data encoding among LG modes with different p values [23].

In this Letter, we experimentally demonstrate a 10 Mbit/s free-space quantum communication link by encoding data on orthogonal LG modes with different p indices. By encoding data on two $LG_{\ell p}$ modes (i.e., for $\ell = 0$, we encode ["0", "1"] as [$p = 0$, $p = 1$], and for $\ell = 1$, we encode ["0", "1"] as [$p = 0$, $p = 1$]), the quantum symbol error rate (QSER) <5% is achieved at an encoding rate of 10 Mbit/s. Moreover, we also investigate the influence of the circle radius (R) of the receiver phase pattern on registered photon rates and the QSER. The results show that a receiver phase pattern whose R does not match the beam size of the LG modes would induce higher cross talk between the two quantum branches.

Figure 1 shows the concept of quantum data encoding based on two $LG_{\ell p}$ modal sets, each having the same ℓ and

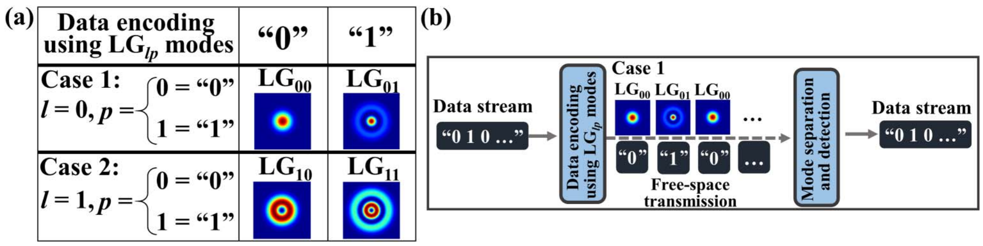

Fig. 1. (a) Two $LG_{\ell p}$ modes with the same ℓ but different p values for data encoding (case 1: LG_{00} and LG_{01}; case 2: LG_{10} and LG_{11}). (b) Concept of quantum data encoding based on two $LG_{\ell p}$ modes.

different p values (LG_{00} and LG_{01} or LG_{10} and LG_{11}). For quantum data encoding, photons are encoded by converting each photon into a specific $LG_{\ell p}$ mode from an $LG_{\ell p}$ modal set with the same ℓ and different p. Within each symbol period, every single photon exists in only one of the two $LG_{\ell p}$ modes. After the free-space transmission followed by the mode separation and detection, the data stream could be recovered with low inherent cross talk due to the orthogonality of the different $LG_{\ell p}$ modes.

The experimental setup of quantum encoding using two LG modes with the same ℓ and different p is shown in Fig. 2. Two pseudorandom sequences, generated by an arbitrary waveform generator (AWG), are first amplified and then used to directly modulate two 850 nm lasers, respectively. The two branches (branch ① and branch ②) are then coupled into two collimators, each of which emits a collimated Gaussian beam with a diameter of 3.99 mm. Two programmable spatial light modulators (SLMs) loaded with different phase holograms on the screens are used to convert the two incoming beams into the desired LG beams (LG_{00} and LG_{01} or LG_{10} and LG_{11}). A beam splitter (BS) is used to spatially combine the two $LG_{\ell p}$ beams. Then the combined beams are attenuated by an attenuator to the single-photon level. The resulting quantum channel propagates in free space in the lab over ~1 m.

After free-space transmission, the incoming quantum channel is split into two copies by another BS and then sent to SLM-3 and SLM-4. These SLMs are loaded with the designed phase patterns to convert the $LG_{\ell p}$ photons back into Gaussian-like (LG_{00}) photons simultaneously. Each of the downconverted photons is coupled into a single-mode fiber (SMF) using two lenses and collimators. The two branches are simultaneously detected by single-photon detectors (SPDs) that have a deadtime of 50 ns and an afterpulsing probability of 0.5%. When a photon event is detected by the SPD, a 25-ns-wide pulse would be generated. All the output pulses produced by SPDs are sampled and recorded by a real-time oscilloscope with a sampling rate of 250 Msample/s. Finally, offline digital signal processing (DSP) is used to calculate the QSER and the registered photon rate [24].

Figure 3(a) presents the normalized waveforms of the two branches and their combination at the transmitter. Here, the transmitted symbol rate is 10 Mbit/s, and the signal duty ratio is 25%. The combined waveform verifies that the photons exist in only one of the two branches in each 100 ns period. At the receiver side, the attenuated signals are detected by the SPDs, as shown in Fig. 3(b). The mode set we use here is LG_{00} and LG_{01}, and we observe that only one of the two LG modes is active in each symbol period.

Figures 4(a1) and 4(a2) show the experimental intensity profiles of the LG_{00} and LG_{01} beams, respectively, in the classical domain. Figures 4(a3) and 4(a4) show the specific phase patterns loaded on the screens of SLM-3 and SLM-4, respectively, to downconvert the incoming LG_{00} and LG_{01} photons into Gaussian-like (LG_{00}) photons. We note that the receiver phase pattern for the LG_{00} mode is an all-zero phase pattern, while the one for the LG_{01} mode contains a circle inside with a π phase difference from the outside.

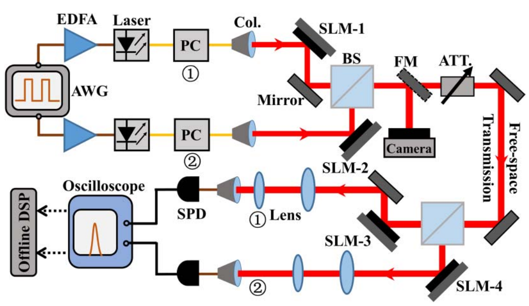

Fig. 2. (a) Experimental setup of a quantum communication link based on $LG_{\ell p}$ modes. AWG, arbitrary waveform generator; PC, polarization controller; Col., collimator; SLM, spatial light modulator; BS, beam splitter; FM, flip mirror; ATT, attenuator; SPD, single photon detector; DSP, digital signal processing.

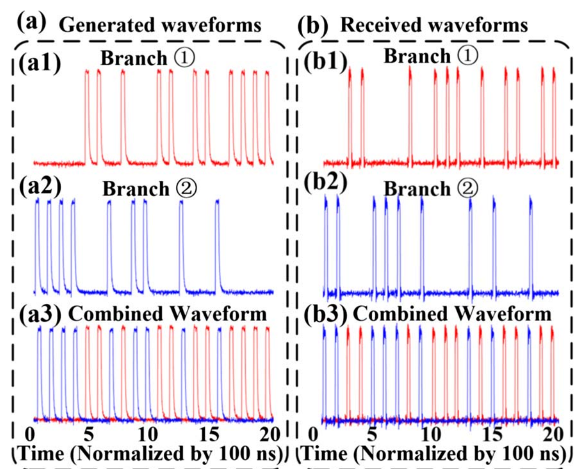

Fig. 3. (a) Normalized generated waveforms of the two branches [(a1) and (a2)] and their combination (a3) at the transmitter. (b) Normalized waveforms of the two branches and their combination received by SPDs using the mode set {LG_{00} and LG_{01}}. The symbol period is 100 ns.

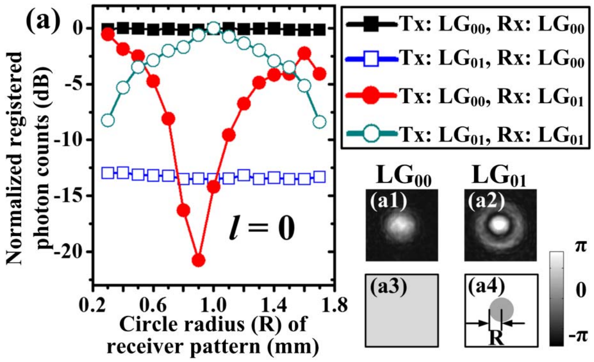

Fig. 4. Cross talk analysis between LG_{00} and LG_{01} modes as a function of the circle radius (R) of the receiver pattern using the quantum measurement approach. (a1) and (a2) Experimental intensity profiles of the LG_{00} and LG_{01} modes in the classical domain. (a3) and (a4) Receiver phase patterns for LG_{00} and LG_{01} modes. Tx, LG_{00}; Rx, LG_{00}. LG_{00} is transmitted, and LG_{00} is received. The optimized R value is 0.9 mm.

The radius of the circle (R) in the receiver phase pattern for the LG_{01} mode might affect the power loss for LG_{01} mode and the cross talk between the LG_{00} and LG_{01} modes. Therefore, in order to achieve an optimized system performance, the R of the receiver phase pattern is required to match the beam size of the received LG_{01} mode [19]. Here, based on the quantum measurement approach, different R values are tested, and the normalized registered photon counts are measured by SPDs and an oscilloscope, as shown in Fig. 4(a). Each value is measured as a ratio of the measured photon counts (power) to the maximum photon counts (power) in this figure in a unit of dB. We note that when receiving LG_{00} photons, the registered photon counts remain relatively stable. We think this is due to the fact that the receiver pattern for LG_{00} photons is an all-zero phase pattern, and may not be sensitive to the beam size. However, when receiving LG_{01} photons, the lowest cross talk between LG_{00} and LG_{01} photons (<20 dB), as well as the minimum photon loss for LG_{01} photons, is achieved when R is 0.9 mm, while the photon loss and the cross talk will become higher for other R values.

Figures 5(a1)–5(a3) show the cross talk matrices between the LG_{00} and LG_{01} modes for $R = 0.5$, 0.9, and 1.3 mm, respectively. We see that for $R = 0.5$ or 1.3 mm, the photon loss and cross talk between the LG_{00} and LG_{01} modes are higher, which might degrade the system performance. Figures 5(b) and 5(c) present the registered photon rates and QSERs for the various R values as a function of average photon number per pulse (μ) for the LG_{00} and LG_{01} modes. Due to the dead time limitation of our SPDs, a transmitted data rate of 10 Mbit/s is chosen. Results indicate that compared with the case of $R = 0.9$ mm, the registered photon rate is lower, and the QSER becomes higher when $R = 0.5$ or 1.3 mm. We think this degradation is due to the higher photon loss and cross talk caused by the mismatch between R and the beam size of the LG_{01} modes. We observe even for $R = 0.9$ mm, the registered photon rate at a μ of 1 is lower than the transmitted data rate (10 Mbit/s). This is mainly due to the limited photon detection efficiency of our SPDs (45% at 850 nm).

Besides the case of LG modes with $\ell = 0$, we also investigate the orthogonality of LG modes with higher ℓ ($\ell = 1$) and

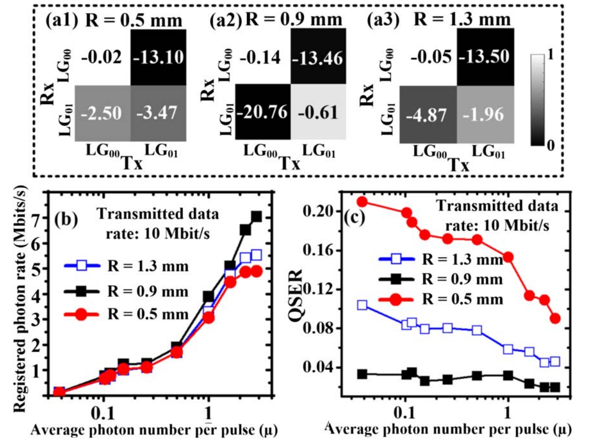

Fig. 5. (a1)–(a3) Cross talk matrices between LG_{00} and LG_{01} modes for different R values. (b) Registered photon rates and (c) QSERs with different R values with average photon number per pulse (μ).

different p ($p = 0$ or 1) values. Figures 6(a1) and 6(a2) present the experimental intensity profiles of LG_{10} and LG_{11} beams, respectively, in the classical domain. Figures 6(a3) and 6(a4) show the receiver phase patterns, which are utilized to down-convert LG_{10} and LG_{11} modes into Gaussian-like (LG_{00}) photons, respectively. Here, for LG_{10} modes, the receiver phase pattern is only a special spiral phase pattern. However, for LG_{11} modes, the receiver phase pattern also has a circle at the center, which is similar to the one for the LG_{01} mode. Moreover, the inside and outside sections of the circle have a π phase difference. Figure 6(a) presents the effect of R values on the normalized registered photon counts, which shows a trend similar to the one using the LG_{00} and LG_{01} modes. We observe that the cross talk between LG_{10} and LG_{11} photons also achieves its minimum value of ∼ – 14 dB at $R = 0.9$ mm.

Figures 7(a1)–7(a3) shows cross talk matrices between the LG_{10} to LG_{11} modes when $R = 0.5$, 0.9, and 1.3 mm. The cross talk and power loss for $R = 0.9$ mm are lower than the cases of $R = 0.5$ or 1.3 mm. The registered photon rates and QSERs with different R are shown in Figs. 7(b) and 7(c).

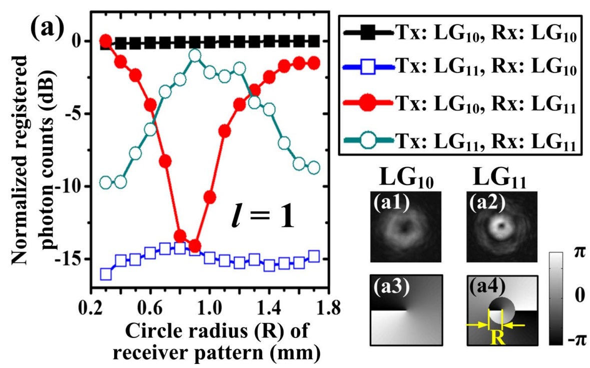

Fig. 6. Cross talk analysis between LG_{10} and LG_{11} modes with R of the receiver pattern using the quantum approach. (a1) and (a2) Experimental intensity profiles of the LG_{10} and LG_{11} modes in classical domain. (a3) and (a4) Receiver phase patterns for the LG_{10} and LG_{11} modes.

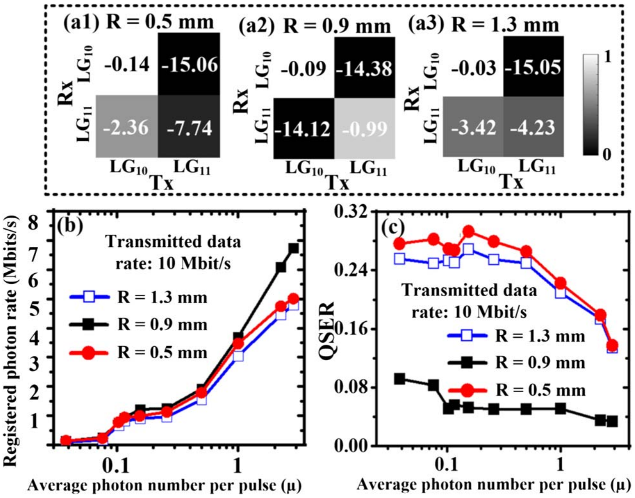

Fig. 7. (a1)–(a3) Cross talk matrices between LG_{10} and LG_{11} modes for different R values. (b) Registered photon rates and (c) QSERs with different R of the receiver phase pattern with μ.

When $R = 0.5$ or 1.3 mm, a lower registered photon rate and a higher QSER are observed, which is consistent with cross talk behaviors mentioned above.

We experimentally demonstrate a quantum communication link using data encoding on orthogonal LG modes. The utilization of LG modes with different p values could potentially provide more communication modes over systems with only $p = 0$ modes [18]. In our experiment, the proof-of-concept quantum link is over a short ∼1 m in the lab. However, when considering propagation over a longer distance, atmospheric turbulence might affect the system performance in terms of photon loss as well as increasing the probability of the photon coupling to other modes and degrading the QSER [27,28]. In order to reduce the photon loss and QSER, an adaptive optics system might be effective in mitigating the effects of turbulence [28,29].

Funding. National Science Foundation (NSF) (ECCS-1509965); Vannevar Bush Faculty Fellowship program sponsored by the Basic Research Office of the Assistant Secretary of Defense for Research and Engineering and funded by the Office of Naval Research (ONR) (N00014-15-1-2635, N00014-16-1-2813).

REFERENCES

1. N. Gisin, G. Ribordy, W. Tittel, and H. Zbinden, Rev. Mod. Phys. **74**, 145 (2002).
2. C. Bennett and G. Brassard, in *International Conference on Computers, Systems & Signal Processing*, Bangalore, India (1984), p. 175.
3. H. Takenaka, A. Carrasco-Casado, M. Fujiwara, M. Kitamura, M. Sasaki, and M. Toyoshima, Nat. Photonics **11**, 502 (2017).
4. N. Namekata, H. Takesue, T. Honjo, Y. Tokura, and S. Inoue, Opt. Express **19**, 10632 (2011).
5. A. R. Dixon, Z. L. Yuan, J. F. Dynes, A. W. Sharpe, and A. J. Shields, Opt. Express **16**, 18790 (2008).
6. H. Bechmann-Pasquinucci and W. Tittel, Phys. Rev. A **61**, 062308 (2000).
7. N. J. Cerf, M. Bourennane, A. Karlsson, and N. Gisin, Phys. Rev. Lett. **88**, 127902 (2002).
8. D. V. Sych, B. A. Grishanin, and V. N. Zadkov, Phys. Rev. A **70**, 052331 (2004).
9. S. P. Walborn, D. S. Lemelle, M. P. Almeida, and P. H. S. Ribeiro, Phys. Rev. Lett. **96**, 090501 (2006).
10. A. Mair, A. Vaziri, G. Weihs, and A. Zeilinger, Nature **412**, 313 (2001).
11. M. Krenn, J. Handsteinera, M. Fink, R. Fickler, and A. Zeilinger, Proc. Natl. Acad. Sci. USA **112**, 14197 (2015).
12. F. M. Spedalieri, Opt. Commun. **260**, 340 (2006).
13. G. Vallone, V. D'Ambrosio, A. Sponselli, S. Slussarenko, L. Marrucci, F. Sciarrino, and P. Villoresi, Phys. Rev. Lett. **113**, 060503 (2014).
14. M. Mirhosseini, O. S. Magaña-Loaiza, M. N. O'Sullivan, B. Rodenburg, M. Malik, M. P. J. Lavery, M. J. Padgett, D. J. Gauthier, and R. W. Boyd, New J. Phys. **17**, 033033 (2015).
15. R. L. Phillips and L. C. Andrews, Appl. Opt. **22**, 643 (1983).
16. H. C. Kim and Y. H. Lee, Opt. Commun. **169**, 9 (1999).
17. J. Wang, J.-Y. Yang, I. Fazal, N. Ahmed, Y. Yan, H. Huang, Y. Ren, Y. Yue, S. Dolinar, M. Tur, and A. E. Willner, Nat. Photonics **6**, 488 (2012).
18. G. Xie, Y. Ren, Y. Yan, H. Huang, N. Ahmed, L. Li, Z. Zhao, C. Bao, M. Tur, S. Ashrafi, and A. E. Willner, Opt. Lett. **41**, 3447 (2016).
19. A. Trichili, A. B. Salem, A. Dudley, M. Zghal, and A. Forbes, Opt. Lett. **41**, 3086 (2016).
20. K. Pang, H. Song, Z. Zhao, R. Zhang, H. Song, G. Xie, L. Li, C. Liu, J. Du, A. F. Molisch, M. Tur, and A. E. Willner, Opt. Lett. **43**, 3889 (2018).
21. G. Gibson, J. Courtial, M. J. Padgett, M. Vasnetsov, V. Pas'ko, S. M. Barnett, and S. Franke-Arnold, Opt. Express **12**, 5448 (2004).
22. A. J. Willner, Y. Ren, G. Xie, Z. Zhao, Y. Cao, L. Li, N. Ahmed, Z. Wang, Y. Yan, P. Liao, C. Liu, M. Mirhosseini, R. W. Boyd, M. Tur, and A. E. Willner, Opt. Lett. **40**, 5810 (2015).
23. K. Pang, C. Liu, G. Xie, Y. Ren, Z. Zhao, R. Zhang, Y. Cao, J. Zhao, L. Li, H. Song, H. Song, M. Tur, R. W. Boyd, and A. E. Willner, in *Conference on Lasers and Electro-Optics* (2018), paper FTu3G. 4.
24. Y. Ren, C. Liu, K. Pang, J. Zhao, Y. Cao, G. Xie, L. Li, P. Liao, Z. Zhao, M. Tur, R. W. Boyd, and A. E. Willner, Opt. Lett. **42**, 4881 (2017).
25. Y. Zhou, M. Mirhosseini, D. Fu, J. Zhao, S. M. H. Rafsanjani, A. E. Willner, and R. W. Boyd, Phys. Rev. Lett. **119**, 263602 (2017).
26. A. Sit, F. Bouchard, R. Fickler, J. Gagnon-Bischoff, H. Larocque, K. Heshami, D. Elser, C. Peuntinger, K. Günthner, B. Heim, C. Marquardt, G. Leuchs, R. W. Boyd, and E. Karimi, Optica **4**, 1006 (2017).
27. G. A. Tyler and R. W. Boyd, Opt. Lett. **34**, 142 (2009).
28. C. Liu, K. Pang, Y. Ren, J. Zhao, G. Xie, Y. Cao, H. Song, Z. Zhao, H. Song, L. Li, R. Zhang, J. Du, S. M. H. Rafsanjani, G. Labroille, P. Jian, D. Starodubov, R. W. Boyd, M. Tur, and A. E. Willner, in *Conference on Lasers and Electro-Optics* (2018), paper FW4F. 5.
29. B. Rodenburg, M. Mirhosseini, M. Malik, O. S. Magaña-Loaiza, M. Yanakas, L. Maher, N. K. Steinhoff, G. A. Tyler, and R. W. Boyd, New J. Phys. **16**, 033020 (2014).